

# Simulation of the Propagation of a Crack in the Fuselage of An Aircraft

João Diogo Candeias

joao.d.candeias@tecnico.ulisboa.pt

Instituto Superior Técnico, Universidade de Lisboa, Portugal

January 2021

The work presented in this paper is within the area of the assessment of the structural integrity of an aircraft, namely through the study of the “Simulation of the Propagation of a Crack in the Fuselage of an Aircraft” under different loading conditions. The work carried out aims to: evaluate the mechanical resistance of a component in the presence of a crack under a in plane biaxial loading; evaluate the growth of a crack for different loading types (phase variation; frequency variation); evaluate which criteria are more suitable to predict the behavior of a crack for a certain load; validate a numerical analysis algorithm for crack propagation in the context of the mechanical behavior of materials. Predicting crack behavior can have a huge impact on both the aircraft's life span and economic conditions. The simulation of the crack propagation under different conditions of initial loading is done with the modeling and design of a cruciform specimen. Biaxial loadings are analyzed with MTS and MSS criteria with the variation of biaxial ratio, phase and frequency, through the evaluation of the stress field in the crack front.

**Keywords:** Crack Propagation, Cruciform Specimen, Biaxial Loads, Numerical Analysis, Fracture of Mechanics, Stress Intensity Factor

## 1 Introduction

The study and analysis of the structural integrity of mechanical components are areas of great importance in engineering due to the faults in the materials. In recent decades, these have been widely developed due to the evolution of knowledge and studies related to numerical methods, as well as fracture mechanics and fatigue [1].

In order to ensure that these components are viable and efficient throughout their useful life, it is essential to guarantee that failures do not occur. For this, it must be taken into account that the durability of the components plays a fundamental role in an initial phase of an engineering project. One of the main problems in these projects concerns the fatigue fracture of the structural

components. It is estimated that the majority of component failures are related to the phenomenon of fatigue [2], as a result of the accumulation of damage associated with the types of loads to which they are subjected. Aerospace metallic components are subjected to complex multiaxial loads, such as proportional, non-proportional, in-phase and out-of-phase biaxial loads [2]. Although numerous efforts have been made to understand in detail the crack propagation under uniaxial loads, few studies have been carried out under biaxial and multiaxial loading conditions. Therefore, it is pertinent to develop a numerical algorithm that allows the simulation of crack propagation in biaxial conditions, which may represent the loading conditions of an aircraft's fuselage. In this context, in the case of this study, a cruciform specimen is used for the in-depth study of crack growth. Throughout this article, different theories of Fracture Mechanics are addressed to understand the influence of different parameters and loads on crack propagation, with special emphasis on the criteria of maximum tangential stress and maximum shear stress, MTS and MSS, respectively.

## **2 Theoretical Concepts**

### **2.1 Structural Failure Modes**

The occurrence of component failures or rupture in aerospace engineering is an extremely important phenomenon and requires some study, which led to the development of this work. To comply with airworthiness requirements, aircraft must be designed to ensure either that any failure is repaired or the component is taken out of service before failure. The aircraft must be

designed to be damage tolerant. In this way, it is essential to know the different modes of structural failure to which the various components are subject, such as creep, buckling, fatigue and corrosion [8].

### **2.2 General Fatigue Review**

Considering the possibility that the structures contain small cracks and the risk that these cracks may continue to propagate through fatigue until the final rupture, it is easy to see the importance of studying the phenomenon of crack propagation. For this, the comprehension of Fracture Mechanics should be understood in detail, as well as the design methodologies that were developed in the scope of the study of fatigue crack growth (FCG). In this way, the concept of crack and how the stress fields vary in the crack front area must be taken into account, specially the stress intensity factors and its influence in the crack propagation [2].

Knowing that a large part of the structural failures of mechanical components is caused by FCG, we can perceive the importance of the phenomenon of fatigue presented. Consequently, the structural integrity of the components during their service life is guaranteed.

### **2.3 Fracture Mechanics**

As previously mentioned, it is important to understand the distribution of the stress field in a crack, especially in the area of the crack front. The singularity presented in this place leads to the formation of a plastic zone. However, in the theory of the MFLE used, this behavior is not taken into account and the tension is given by an ideal crack

according to the linear elastic model. Consequently, this theory reveals some limitations because it does not include the influence of this zone, which may be in the plastic domain. In Fracture Mechanics, the rupture of the components is associated with the growth of cracks. So, it is important to have a thorough knowledge of this phenomenon. Furthermore, it is essential to know the steps related to the fatigue phenomenon. This process begins with nucleation, followed by microscopic growth of the crack(s) and subsequent propagation (perpendicularly to the applied stresses) until its final rupture. Depending on the type and direction of the load applied on a crack, there are three different ways to propagate the crack[1]:

- **Mode I** – Opening mode: the propagation of the crack surfaces proceeds in a perpendicular direction to the loading plane and is caused by the normal applied tensile stresses.
- **Mode II** – Sliding mode: the propagation of the crack surfaces occurs in a parallel direction to the loading plane and originates shear stresses in the plane.
- **Mode III** – Tearing mode: it is characterized by tangent loads outside the crack plane, in the direction of the thickness of the body, and is caused by shear stresses outside the plane.

The stress intensity factors associated to this load modes studied in this work,  $K_I$  e  $K_{II}$  allows to predict the direction of the crack propagation

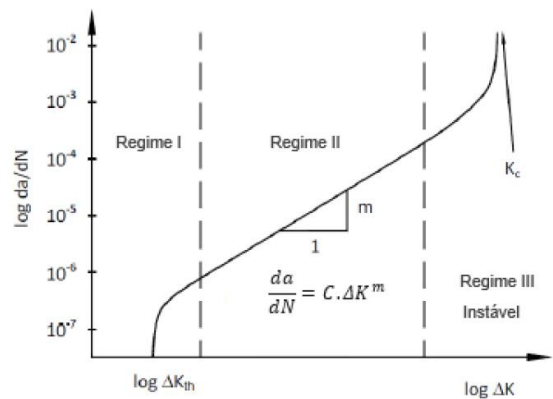


Figure 1 – Crack growth VS Stress Intensity Factor [1]

In the first region (figure 1), the propagation rate is extremely dependent on the variation of the SIFs. In this zone, propagation may not occur, or it could be much reduced. This happens when the critical value is not reached. This region is fundamentally characterized by the influence of the material's microstructure, medium tension and the (environmental) conditions in which it is found. In the second region, there is continuous growth and certain combinations of medium voltage, frequency and (environmental) conditions tend to have a great influence on the propagation. The propagation speed reveals a linear relationship between the SIFs and the crack growth. This relationship is described by the Paris Law,

$$da/dN = C \Delta K^m \quad (1)$$

since C and m are constant in the material and  $\Delta K$  is described by the following expression:

$$\Delta K = Y \Delta \sigma \sqrt{\pi \Delta a} \quad (2)$$

$\Delta\sigma$  represents the variation of applied stresses,  $Y$  is the form factor and  $\Delta a$  the change in the crack size.

In the third region, the propagation speed continues to increase unsteadily until it reaches a critical value of stress  $K_{Ic}$ , depending on the material under study.

This study is focused on the second region of the crack propagation, which follows the Paris Law. The applied criteria and the equations for the crack growth and direction of propagation calculations are briefly explained in the chapter of fatigue crack propagation.

### 3 Material and Methods

#### 3.1 Cruciform Specimen and Initial Crack Geometry

A symmetrical cruciform specimen is used for the biaxial study, as shown in figure 2.

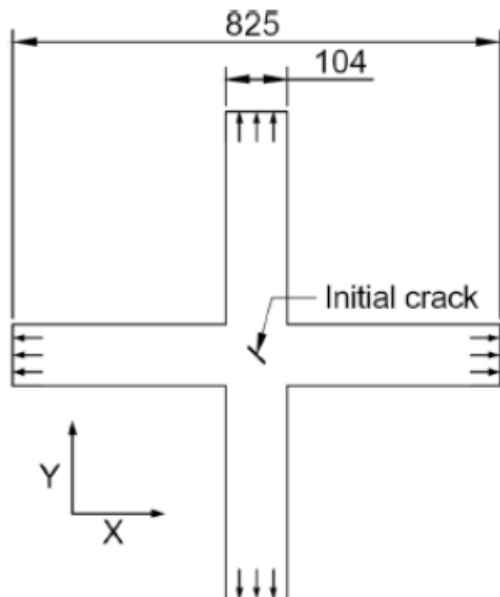


Figure 2 – Cruciform Specimen [4].

The specimen geometry is in accordance to the international program NESC and it was adapted to have a radius of curvature of

10mm between the arms of the specimen. A centered initial crack either aligned or inclined to the load directions is located at the center of the specimen. The inclination angle values of the initial crack examined are  $\beta=0^\circ, 15^\circ, 30^\circ$  and  $45^\circ$ , and the corresponding crack length is  $2a=36$  mm.

#### 3.2 Applied Loading

Prescribed loads  $\sigma_x$  and  $\sigma_y$  were applied to the arms of the specimen. In all loading cases studied, the nominal load applied is 100MPa. In equations 3 and 4 the equations of the loads applied are presented:

$$\sigma_x(t) = \sigma_{med} + \sigma_a \cdot \sin(\omega t + \phi) \quad (3)$$

$$\sigma_y(t) = \sigma_{med} + \sigma_a \cdot \sin(\omega t + \phi) \quad (4)$$

Where,  $\sigma_m$  is the mean stress,  $\sigma_a$  nominal stress,  $\phi$  the phase angle and  $\omega$  the frequency. All load conditions were applied with an 0.1 stress ratio ( $R = S_{min}/S_{max}$ )

The numerical crack paths are obtained with different biaxial ratios, phase angle of  $0^\circ, 90^\circ, 180^\circ$ , and also with  $45^\circ$  in the case of the study of influence of the frequency.

#### 3.3 Numerical Model

Throughout a Matlab numerical algorithm developed by R. Baptista [7], combined with Abaqus, the implementation of the finite element method is employed to model crack propagation. It enables the crack growth simulation without the necessity of creating a new mesh. Inertial effects are not considered, and a small yielding condition is assumed at the crack tip. The material behavior is taken as elastic, with  $E=72$  GPa and  $\nu=0.3$ , in plane strain conditions. The crack is successively propagated in the

following manner: First, stress intensity factors (SIFs) are calculated using the domain independent integral interaction for each crack tip. Then, a fatigue crack propagation criterion is applied (MTS/MSS), and the crack is extended in the predicted direction. The mesh and crack extension sizes and other information about this algorithm that have been analyzed could be consulted in detail in the dissertation.

### 3.4 Fatigue Crack Propagation

In two-dimensional linear-elastic fracture mechanics and under mixed loading conditions that are variable with time, the stress state is given by  $K_I$  and  $K_{II}$  in equation 5 and 6.

$$\sigma_{\theta\theta}(t, \theta) = \frac{K_I(t)}{\sqrt{2\pi r}} \left[ \frac{3}{4} \cos\left(\frac{\theta}{2}\right) + \frac{1}{4} \cos\left(\frac{3\theta}{2}\right) \right] + \frac{K_{II}(t)}{\sqrt{2\pi r}} \left[ -\frac{3}{4} \sin\left(\frac{\theta}{2}\right) - \frac{3}{4} \sin\left(\frac{3\theta}{2}\right) \right] \quad (5)$$

$$\tau_{r\theta}(t, \theta) = \frac{K_I(t)}{\sqrt{2\pi r}} \left[ \frac{1}{4} \sin\left(\frac{\theta}{2}\right) + \frac{1}{4} \sin\left(\frac{3\theta}{2}\right) \right] + \frac{K_{II}(t)}{\sqrt{2\pi r}} \left[ \frac{1}{4} \cos\left(\frac{\theta}{2}\right) + \frac{3}{4} \cos\left(\frac{3\theta}{2}\right) \right] \quad (6)$$

Virtual or equivalent SIF may be calculated (eq 7,8) along a virtual crack extension direction. It allows to predict the crack propagation angle  $\theta$ :

$$K_I^*(t, \theta) = \sigma_{\theta\theta}(t, \theta) \sqrt{2\pi r} = K_I(t) \left[ \frac{3}{4} \cos\left(\frac{\theta}{2}\right) + \frac{1}{4} \cos\left(\frac{3\theta}{2}\right) \right] + K_{II}(t) \left[ -\frac{3}{4} \sin\left(\frac{\theta}{2}\right) - \frac{3}{4} \sin\left(\frac{3\theta}{2}\right) \right] \quad (7)$$

$$K_{II}^*(t, \theta) = \tau_{r\theta}(t, \theta) \sqrt{2\pi r} = K_I(t) \left[ \frac{1}{4} \sin\left(\frac{\theta}{2}\right) + \frac{1}{4} \sin\left(\frac{3\theta}{2}\right) \right] + K_{II}(t) \left[ \frac{1}{4} \cos\left(\frac{\theta}{2}\right) + \frac{3}{4} \cos\left(\frac{3\theta}{2}\right) \right] \quad (8)$$

It should be mentioned that negative values of  $K_I^*$  have no physical meaning (crack face overlap) and are set to 0.

The factors in eq. 7 and eq. 8 are known as virtual stress intensity factors  $K_I^*$  e  $K_{II}^*$  and they allow to predict the angle for crack propagation through the application of the different criteria. That can be based on  $K_{I\max}^*$ ,  $\Delta K_{I\max}^*$  or  $\Delta K_{II\max}^*$  criteria and calculated for different values of  $t$  and  $\theta$ . The maximum tangential stress criteria is given by  $K_{I\max}^*$  and the maximum shear stress is in agreement with  $K_{II\max}^*$ .

## 4 Results Analysis

In general, under proportional loading, a crack kinks in a direction where the tensile normal stress field (mode I stress intensity factor  $K_I^*$ ) is maximum. Besides that, this direction is coincident with the direction of  $K_{II}^*$  is equal to zero, in accordance with the direction of maximum  $\Delta K_I^*$ . [4,8]

Under non-proportional loading, the ratio of the SIF  $K_I/K_{II}$  is not kept constant during the cycle. There are three potential directions of crack orientation: the directions corresponding to  $K_{I\max}^*$  and  $\Delta K_{I\max}^*$ , or in a direction that usually falls between this values. In some cases of propagation, the criteria of  $\Delta K_{II\max}^*$  shows good results for the crack angle, where the crack orientation is the direction for which the shear stress range is maximum. [3]

### 4.1 In phase Proportional

When the loads applied are proportional and in phase, the propagation curves under the different load ratios applied are different and their propagation paths for the three studied load ratios can be seen in Figure 3.

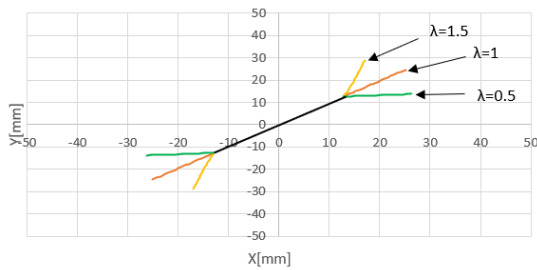


Figure 3 – Propagation curve: biaxial ratio

In figure 4 and 5, the graphs correspond to biaxial ratio of  $\lambda = 0,5$ . These graphics show the variation of the SIF for the first and the second mode of loading, respectively. The maximum and minimum values of  $K_I^*$  and  $\Delta K_{II}^*$  show that the angle of propagation in this graphics is on agreement with the angle of the figure 3, which was obtained in the numerical algorithm.

In the loads studied in this section, the value of the expected propagation angle when the value of  $K_{II}^*$  is null and coincides with the value of maximum  $K_I^*$  means that the crack will grow in the load plane.

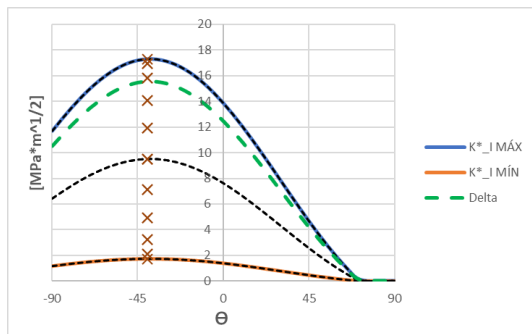


Figure 4 – Stress Intensity Factor  $K_I^*$ :  $\lambda = 0,5$

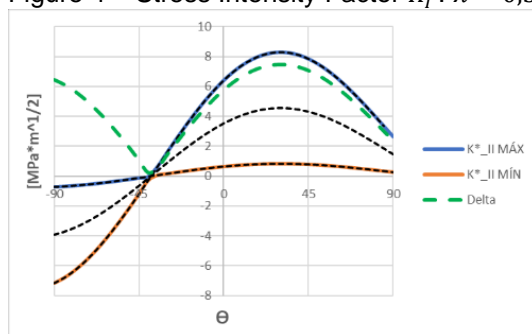


Figure 5 - Stress Intensity Factor  $K_{II}^*$ :  $\lambda = 0,5$

It was also studied the initial crack aligned with the horizontal with a propagation curve corresponding to the three loading ratios applied:  $\lambda = 0.5$ ;  $\lambda = 1$ ;  $\lambda = 1.5$ . In this case, changing the applied load ratios does not change the crack's propagation path. In this way, according to the MTS criterion used, the graphs of variation of the stress intensity factors presented are also the same. In this study, the crack growth values are variable and pre-defined in the program as a function of the number of cycles. The figure 6 shows how the horizontal gap grows along the applied loading cycles. It is evident in this figure that as the gap spreads, its growth rate increases. This is calculated through the Paris Law.

The importance of carrying out non-destructive inspections and the existence of a damage-tolerant design (suitable for the various components of the aircraft) should be highlighted, to avoid the occurrence of crack propagations and to minimize failures within its period of operation.

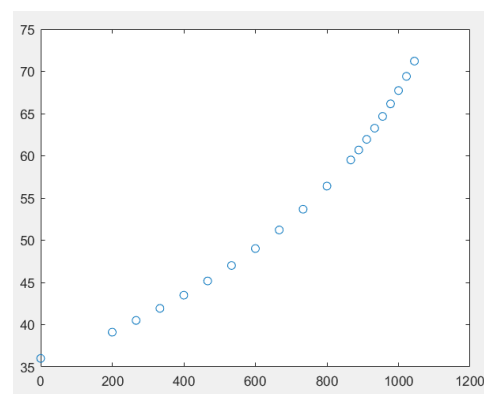


Figure 6 – Crack growth VS Number of Cycles

The propagation curves presented were obtained in the numerical algorithm used, according to the MTS criterion. The different propagation paths can be observed,

depending on the different initial conditions of the crack we are analyzing.

#### 4.2 Out of Phase

In order to analyze the influence of the loading phase and also the different criteria used two simulations for each loading / initial crack angle combination were performed. In one of them, we use the MTS criterion. In the other, we use the MSS criterion.

In figure 7 and 8, the blue line corresponds to the load applied when the initial angle is 15°. The orange and green lines correspond to the loads where the crack is inclined at 30° and 15°, respectively. MTS and MSS criteria were applied with and out-of phase 90° loading.

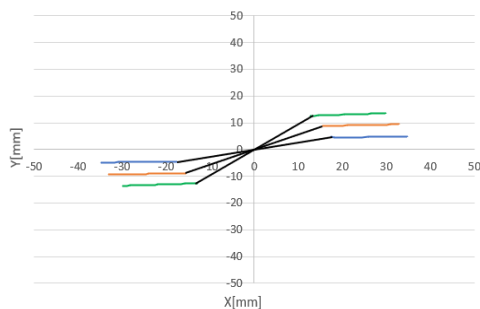


Figure 7 - Propagation curve:  $\phi = 90^\circ$ , MTS

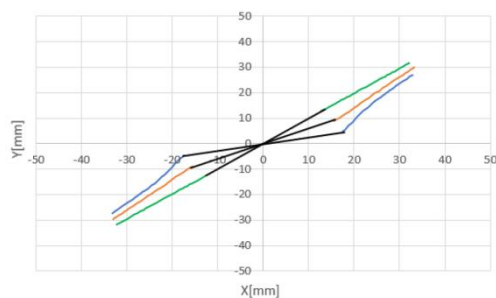


Figure 8 – Propagation curve:  $\phi = 90^\circ$ , MSS

After presenting the propagation curves obtained in the algorithm for the different

initial crack angles, it is essential to show the graphs of variation of the stress intensity factors obtained for each case. In figure 9 and 10 show the variation of the stress intensity factor  $K_I^*$  and  $K_{II}^*$  maximum and minimum, respectively, with out of phase 180° loading.

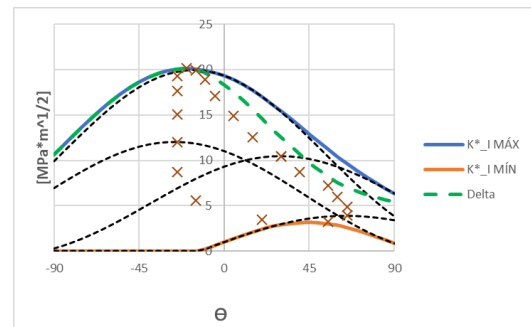


Figure 9 - Stress Intensity Factor:  $K_I^*$

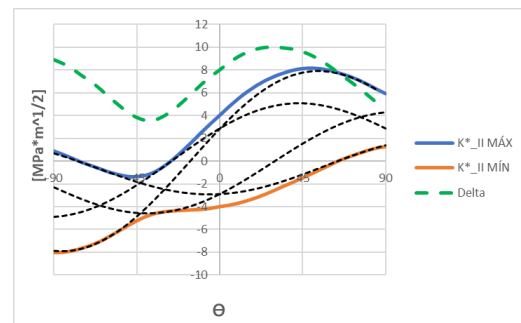


Figure 10 – Stress Intensity Factor:  $K_{II}^*$

The results for the propagation angle obtained by the application of criteria MTS and MSS are different.

To understand the influence of the difference of phase there are presented the next graphics obtained in the algorithm, in accordance with MTS and MSS, respectively.

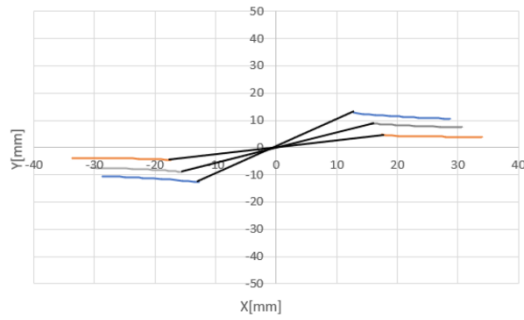


Figure 11- Propagation curve  $\phi = 180^\circ$ , MTS

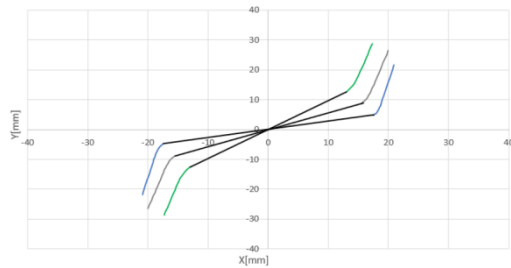


Figure 12- Propagation curve  $\phi = 180^\circ$ , MSS

The angles obtained for the phase of  $180^\circ$  are bigger than the results for the phase of  $90^\circ$ . The angles are different accordingly to which criteria (MTS/MSS) is applied.

In these graphs, the magnitude of the propagation angle value increases as long as the value of the initial angle of the crack increases too and the angles obtained in the algorithm are the same than in the graphics of the variation of SIF. Regarding the graphs of variation of the stress intensity factor  $K_{II}^*$ , it is possible to observe that the value corresponds to the maximum value of  $\Delta K_{II}^*$ . This allows to predict the crack propagation angle, according to the MTS criterion, which decreases as the initial slope of the crack is increased. Thus, to validate these results, the graphs of the variation of the stress intensity factors are compared with the numerical results developed by Garcia et al [8]. When comparing these graphs with those presented for the same loading

conditions, it can be seen that they are very similar to the ones presented in this study. Also, the values of the propagation angles obtained by these authors coincide with the results. In the three simulations carried out in the numerical algorithm for each criterion, when applying out of phase loads, as the gap grows it is possible to verify that the gap tends to align with horizontal direction, according to the MTS, where the values for the crack propagation angle are the same accordingly with the criteria  $K_{I}^* e \Delta K_{I}^*$ . However, according to the MSS criterion ( $K_{II}^*$ ) the slots are aligned with the  $45^\circ$  direction. In both cases the propagation angle decreases with growth of the crack. The propagation angles according to maximum  $\Delta K_{II}^*$  decrease with the increase of the initial crack inclination. In the loads  $180^\circ$  out of phase, for a slope of the initial crack of  $45^\circ$ , the crack propagation simulations were also performed for a load ratio of  $\lambda = 0.5$  and  $\lambda = 1.5$ . It is easy to see that there is a symmetrical change in the angle of propagation obtained for these load ratios. This makes us understand that the load ratio and the phase are one of the most important factors to consider in the study direction of propagation angle.

### 4.3 Frequency Varying

In order to analyze the influence of the different initial loading conditions and the different propagation criteria used with frequency variation, two simulations are performed for each case. One of them uses the MTS criterion and the other the MSS criterion. Graphs of the stress variation intensity factors  $K_I^*$  and  $K_{II}^*$  for each of the cases under study were not presented here.



### 4.3.1 Double Frequency

In general, the results obtained from the curves and the propagation graphs with double frequency and in phase were identical to those obtained in the previous case. In figure 13 and 14, MTS and MSS criteria are applied, respectively, for these conditions. When the angle of the initial crack is  $45^\circ$ , the crack bifurcates and that's why the curve is in another direction.

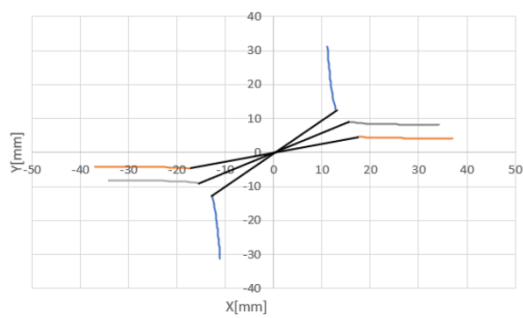


Figure 13 - Propagation curve  $\phi = 0^\circ$ , MTS

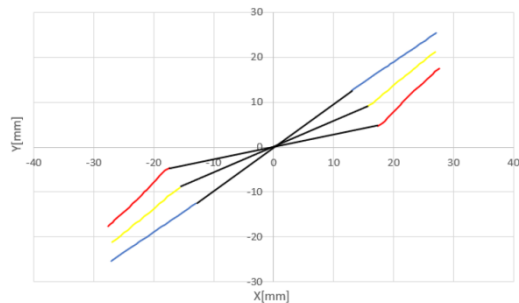


Figure 14 - Propagation curve  $\phi = 0^\circ$ , MSS

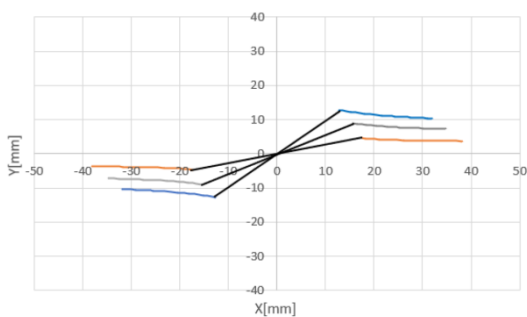


Figure 15 - Propagation curve  $\phi = 45^\circ$ , MTS

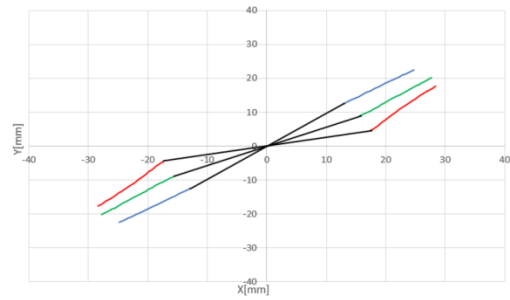


Figure 16 - Propagation curve  $\phi = 45^\circ$ , MSS

As it can be seen, in this case with a  $45^\circ$  offset, the magnitude of the propagation angle is slightly higher according to the maximum  $\Delta K_I^*$  criterion than the maximum  $K_I^*$ . In this context, several authors [4,5] carried out studies aiming to understand which would be the most adequate criterion to predict the direction of propagation of the crack. The conclusion was that the angle of propagation is included among these criteria. In this way, the modulus of the propagation angle of a crack under loading conditions with double frequency on the horizontal axis and a phase difference of  $45^\circ$  is slightly higher than the case without offset and with the same frequencies, according to the MTS criterion. As for the MSS criterion, or parameter that maximizes  $\Delta K_{II}^*$ , in this case of loading, the propagation angles obtained were higher than those of loading without lag and with the same frequency.

### 4.3.2 Static Load

For loads with zero frequency on the horizontal axis (static load), the same crack inclinations ( $15^\circ$ ,  $30^\circ$ ,  $45^\circ$ ) were studied, through the propagation results of the numerical algorithm and the graphs of the SIFs were obtained under these loading conditions (figure 17 and 18).

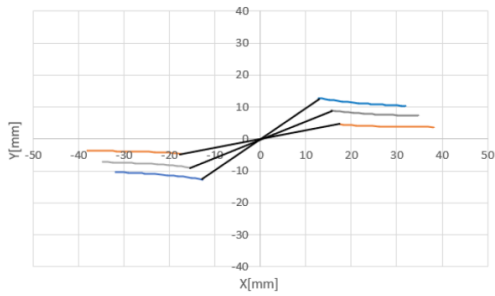


Figure 17 - Propagation curves, MTS

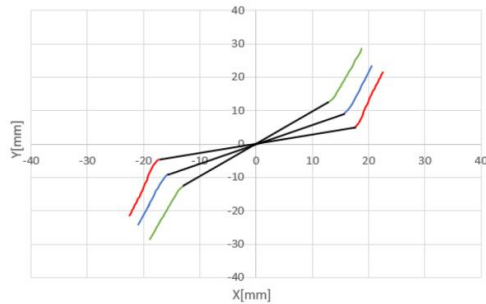


Figure 18 - Propagation curves, MSS

In this case, where static load is applied to the horizontal axis has zero frequency, the maximum  $\Delta K_I^*$  criterion coincides with the maximum  $K_I^*$  criterion, which is the reason why the angles obtained are lower than the double frequency case.

As for loads with zero frequency on the horizontal axis (static load), the solutions of the propagation angle module in this case were lower, in relation to cases where the frequency is doubled, according to the MTS and MSS criteria.

## 5. Conclusions

The study was carried out with conditions of biaxial loadings in the plane. It is important to have knowledge about the fracture mechanics and the stress intensity factors, in order to calculate the angle of propagation of a crack. Also, damage-tolerant design and nondestructive inspections are the keys to ensure the airworthiness. The numerical

results agree with the results found in the literature. It can be concluded that crack paths predicted using different orientation criteria, such as  $\Delta K_{I_{m\acute{a}x}}$ ,  $K_{I_{m\acute{a}x}}$  and  $\Delta K_{II_{m\acute{i}n}}$ , can be different from each other. Further, experimental tests should be carried out in order to confirm these result.

## 5. References

- [1] Santos, T. 'Estudo numérico da propagação de fendas de fadiga num aço de alta resistência', tese IST, 2017
- [2] Hopper C. 'Fatigue crack propagation in biaxial stress fields', J Strain Anal Eng. Des., 1977
- [3] Breitbarth, E. Besel, M. 'Fatigue crack deflection in cruciform specimens subjected to biaxial loading Conditions', Elsevier, vol. 113, 345-350, 2018
- [4] Garcia, D. 'Analysis of the effect of out-of-phase biaxial fatigue loads on crack paths in cruciform specimens using XFEM', vol. 123, páginas 87-95, 2019
- [5] Breitbarth, E., 'Testing of cruciform specimens representing characteristics of a metallic airplane fuselage section', volume 108, páginas 116-126, 2018
- [6] Neeurukatti, R.K. 'Fatigue crack propagation under in-phase and out-of-phase biaxial loading, Elsevier, vol. 41, 2017
- [7] Baptista, R. 'Algorithm for automatic fatigue crack growth simulation on welded high strength steels', Elsevier, vol. 17, páginas 547-554, 2019
- [8] [ F. Grandt, Damage Tolerant Design and Nondestructive Inspection -Keys to Aircraft Airworthiness, Jr. - ISAA 2011)